



HAL
open science

Nonlinear Negative Resistance-based Harmonic Backscatter

Karan Gumber, Francesco Amato, Corinne Dejous, Simon Hemour

► **To cite this version:**

Karan Gumber, Francesco Amato, Corinne Dejous, Simon Hemour. Nonlinear Negative Resistance-based Harmonic Backscatter. 2020 IEEE/MTT-S International Microwave Symposium (IMS 2020), Aug 2020, Los Angeles, CA, United States. pp.603-606, 10.1109/IMS30576.2020.9223877 . hal-04559977

HAL Id: hal-04559977

<https://hal.science/hal-04559977v1>

Submitted on 26 Apr 2024

HAL is a multi-disciplinary open access archive for the deposit and dissemination of scientific research documents, whether they are published or not. The documents may come from teaching and research institutions in France or abroad, or from public or private research centers.

L'archive ouverte pluridisciplinaire **HAL**, est destinée au dépôt et à la diffusion de documents scientifiques de niveau recherche, publiés ou non, émanant des établissements d'enseignement et de recherche français ou étrangers, des laboratoires publics ou privés.

Nonlinear Negative Resistance-based Harmonic Backscatter

Karan Gumber^{#1}, Francesco Amato[§], Corinne Dejous[#], and Simon Hemour^{#2}

[#]IMS Research Center, University of Bordeaux, CNRS, Bordeaux INP, IMS, UMR 5218, Talence, France

[§]University of Tor Vergata, Rome, Italy

¹karan.gumber@u-bordeaux.fr, ²simon.hemour@u-bordeaux.fr

Abstract— Backscattering communication is a key feature that will enable the true IoT/5G revolution towards massive use. However, the specification pressure it puts on the reader/gateway is a major drag on their deployment. In fact, self-jamming resulting from backscattering operation is highly problematic. Harmonic Backscattering Communication comes as a great solution to improve the dynamic range of the backscattered signal that can be received/analysed, thus increasing communication distance. We propose here a harmonic backscattering front-end based on nonlinear negative resistance device that also operates like usual backscatter tag with legacy reader. The circuit provides above +20dB conversion gain and reflection gain, and operates with a supply voltage below 200mV, which is a critical improvement over transistor technology.

Keywords—Nonlinear device, backscattering, negative resistance, RFID.

I. INTRODUCTION

Backscattering-based wireless communication systems are key for the deployment of billions of devices that will connect the physical world to a digital infrastructure of data. Generally, one interrogator (*e.g.*: a reader, a gateway) can communicate with several low-cost backscattering nodes (*e.g.*: the tags) at once. Backscattering nodes are inexpensive, they rely on few hardware components, and can operate without any batteries. Researchers and entrepreneurs have steadily contributed, during the last decade, in overcoming the limits associated to this technology by improving the communications ranges [1], [2] or by increasing the energy harvesting efficiency [3]-[4].

In most readers, the same antenna is shared by the transmitting and the receiving modules that, if not well isolated, generate self-interference (SI) that can corrupt the signal received by the tag [5]. The interference cancellation circuit is bulky and expensive, which is a drag on the pervasive development of readers. Alternatively, SI can be significantly reduced by employing dual-band architectures in which the reader transmits and receives at different frequencies. Recently, harmonic tag architectures have been documented [6]-[8], while commercial dual-band backscattering systems are already approved by the Federal Communications Commissions (FCC) and available. Nonetheless, a dual-band backscattering approach requires the reflection of higher order harmonics whose generation comes at the cost of high conversion losses that can significantly reduce the communication distance.

The low power sensitivity of tunnel diodes (-50 dBm) and their long-term stability [9] makes them suitable for field use in

long-range backscattering communications. For this reason, tunnel diode has been revived recently for its use in battery-less transponder [10]. After characterizing tunnel diode model AI301A, this paper shows the design process and the experimental results of the Nonlinear Negative Resistance-based Harmonic backscatter front-end.

The monostatic antenna configuration is often used in commercial RFID readers, where transmitter (Tx) and receiver (Rx) share the same antenna. It suffers from low Tx to Rx isolation due to contiguous intra-band operation that results in SI. The jamming signal that leaks from Tx to Rx is mixed with the local oscillator (LO) signal, which results in a large DC component that dominates the down converted tag signal by several order of magnitude. The SI saturates the front end of the system and also propagates the phase noise of the LO to the Rx that can easily corrupt the tag information

A number of techniques have been proposed in the literature so far that compensates the self-jamming before it reaches the receiver front end. It can either be compensated by means of directional coupler or quasi-circulator [11] to differentiate the unmodulated transmitted signal which exhibit high power from the weak backscatter signal. However, circulator can provide maximum 25-30 dB isolation to the transmitted signal from the backscatter signal. The reflection due to the transmit antenna can directly pass through the circulator or directional coupler and dominate the weak backscatter signal. Therefore, the problem of SI can be mitigated by separating the Tx/Rx frequencies, similar to the Frequency-division duplex system. The Tx leakage that influences the Rx frequency is filtered at Tx output, similarly, the leakage outside the Rx frequency is filtered at Tx input. Therefore, in recent years, an alternative solution has been discovered by exploiting the nonlinearity in the RFID tags to generate harmonics for enabling communication.

II. TUNNEL DIODE VERSATILITY

Tunnel diodes have recently seen a new emerging interest for IoT/active antenna devices. In fact, by looking at their characteristic curve (Fig. 1), it is possible to see how many applications can be targeted by the different biasing regions (given small RF signals). For example, at low biases, the tunnel diode can be used as an ‘ON’ switch; in the non-linear regions it can be used as a mixer, and, when the resistance is maximum, as an ‘OFF’ switch. Finally, in the linear negative resistance region, it can be used as low-power amplifier [12].

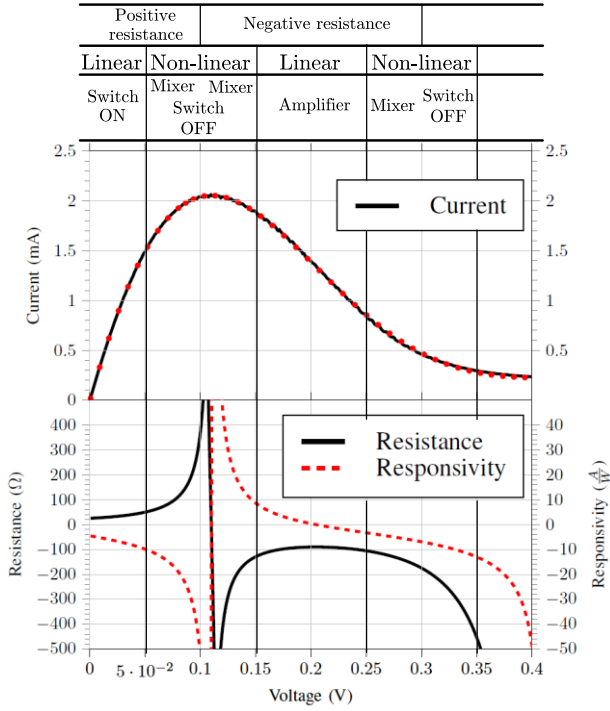


Fig. 1 - Measured DC power and current of the tunnel diode model AI301A with the possible regions of operation. The polynomial fitting of the measured $I(v)$ characteristic allowed to estimate both the differential resistance and the responsivity: $R_d = -120 \Omega$, $\beta(v) = 8 \text{ A/W}$ for biasing at 155 mV.

Measuring the DC characteristic curve, $I(v)$, of tunnel diodes is the first step to experimentally analyse and design tunnel diode-based devices. For this curve, certain performance metrics can be extracted: for example, the differential resistance $R_d(v)$ and current responsivity $\beta(v)$ will be calculated from the $I(v)$ data using central difference approximation derivatives. For high precision extraction of voltage and current consumption of tunnel diode model AI301A, the digital multimeter 34410 (NPLC=10) and the precision biasing supply E3648A on an ENA5080A Test-set (Keysight) were used to measure the current and to bias the diode (1 mV step, step delay of 3 seconds).

A polynomial fit of the characteristic curve was obtained using the least square regression:

$$I(v) = \sum_{i=0}^{i=N} a_i v^i, \quad N \in \mathbb{N}.$$

The 7th order polynomial fitting was extrapolated:

$$I(v) = -5.83v^7 + 14.12v^6 - 12.87v^5 + 5.10v^4 - 0.53v^3 - 0.18v^2 + 0.04v - 1.47 \cdot 10^{-5}$$

from which the corresponding differential resistance and responsivity were computed (Fig. 1). As shown in the $I(v)$ curve, there is a non-linear region for biasing level of 155 mV at which corresponds a current of 1.7 mA, a differential resistance R_d of -120Ω and a responsivity $\beta(v)$ of 8 A/W.

Aimed at solving the SI issue, the Doubler Reflection Amplifier (DRA) concept is illustrated in Fig. 2, where the tunnel diode is employed as a nonlinear element. The signal illuminates the tag at fundamental frequency (f_0), and the non-

linear element in the tag generates and re-radiate the signal back to the reader, both at fundamental frequency and at second harmonic ($2f_0$).

III. NONLINEAR NEGATIVE RESISTANCE CIRCUIT DESIGN

The study of a tunnel diode as a nonlinear component is carried out in Advance Design System (ADS) using a symbolically defined device model. It is an equation-based model that can simulate a nonlinear device's behaviour, both the small- and large-signal, without using a source code. The 7th order polynomial equation, $I(v)$, is used to achieve an accurate DC simulation or harmonic balance simulation of tunnel diode. The distant communications are only possible if the tunnel diode amplifier is able to provide high reflective gain and simultaneously disable the oscillatory conditions. The working principle of DRA is similar to the tunnel diode oscillator, because in both of them the desired gain is obtained by exploiting the negative resistance of tunnel diode. In DRA, there is a challenge in controlling the circuit stability, which means obtaining the desired gain, without, however fulfilling the oscillation condition. The operation of tunnel diode as dual-band amplifier is configured in Fig. 2, where two LC matching circuits are employed in the DRA for dual-band matching.

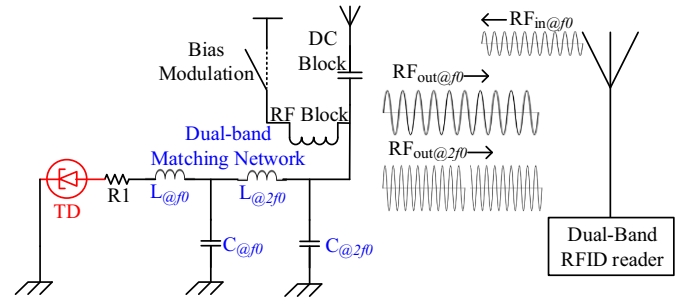


Fig. 2. The nonlinear negative resistance-based harmonic backscatter using commercial tunnel diode.

A series resistance ($R1$) is placed between the tunnel diode and matching circuit to enhance the amplifier reflection gain. The value of series resistance is chosen in such a way that the net positive resistance of the circuit is slightly more than the negative resistance of the tunnel diode. The amplifier yields lower reflection gain if the net positive resistance in the circuit is less than the negative resistance of tunnel diode. For demonstration, the DRA prototypes are fabricated and shown in Fig. 3.



Fig. 3. The Harmonic Doubler Reflection Amplifier.

The various components of the DRA are tuned and optimized using harmonic balance and transient simulations in ADS to ensure maximum reflection and conversion gains at fundamental and 2nd harmonic frequency, respectively. The component values of the DRA are listed in Table I.

Table I. Component Values of the Prototype.

C1=5.2 pF	L1=12.55 nH	R1=8.2 Ω
C2=3.2 pF	L2=8.8 nH	

For prototyping and testing, the AI301A soviet tunnel diode is used which is cheap, rugged and easily available. The inductance and resistance used in the design are from Coilcraft Micro spring air core (1606-8_L, 10_L) and ATC (RMR/RMC01) respectively. The amplification capability of the proposed DRA at the 2nd harmonic frequency is tested using E5080 VNA from Keysight, by exploiting its frequency offset mode. The frequency offset mode is set at the receiver by a multiplying factor of two, which helps to extract the conversion gain at 2nd harmonic, with respect to fundamental frequency. Fig. 4 shows the simulated and measured reflection gain, for an input power of -50 dBm.

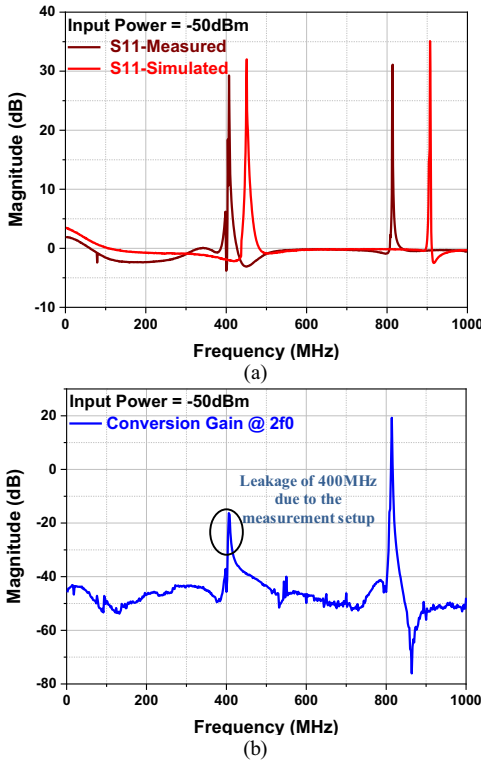


Fig. 4. (a) Simulated and measured reflection amplification at fundamental frequency (b) measured conversion gain at the second-harmonic frequency.

The frequency doubler operation requires impedance matching at both fundamental frequency and 2nd harmonic. Therefore, the whole design process can be done towards S11 only, at both frequencies using the linear simulation tool (S parameter simulation in ADS), instead of heavy nonlinear simulation. A shift in the frequency response is evidenced in Fig. 4 and results from the available components implemented in the prototype.

IV. BACKSCATTERING MODULATION AND BACKSCATTERING HARMONIC MODULATION

A. Steady state operation

By design, the prototype supports 3 types of communication. The fundamental frequency operation, i.e. 450MHz, the legacy operation at 900MHz and the harmonic backscattering operation with a conversion of power from fundamental to 2nd harmonic frequency.

Whereas reflection and conversion gain are both ratios, they originate from different physical mechanisms. The reflection gain is directly due to the small signal (linear) input resistance of the circuit ($Z = -47 - j4 \Omega$ in this case), and is linked to the differential resistance shown in Fig. 1. However, the conversion gain comes from the fast varying (real-time resistance variation) input impedance. As the alternative input voltage swings through the diode IV curve, it sees a different impedance over time. This non-linear process generates harmonics and inter-product modulations (this is used for decades in mixers) and is power dependent, because more received RF power will lead to more impedance variation, hence more conversion.

B. Dynamic bias modulation

The response of the circuit to On-Off-Keying modulation is shown in Fig. 5 with an incoming wave of -50dBm.

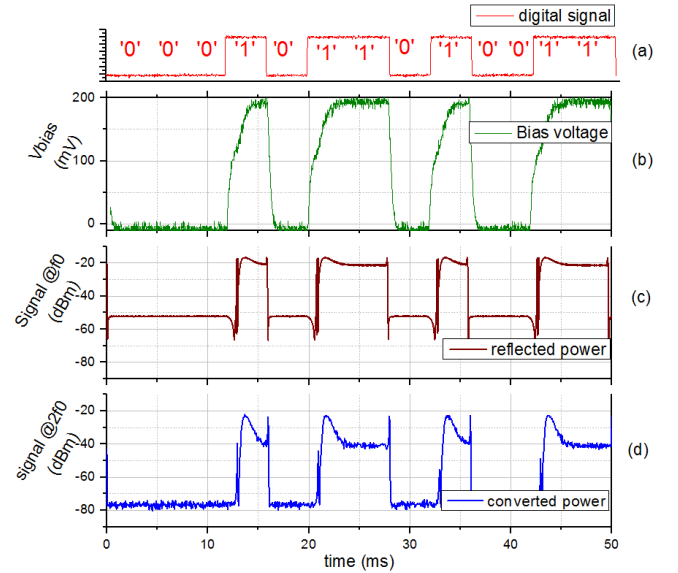


Fig. 5. Time domain input bias and RF output corresponding to an arbitrary bit sequence OOK modulation (a), with an input RF power of -50dBm. (b) Corresponding circuit bias voltage as a function of time (c) output power at $f_0=404$ MHz, the '0' state corresponds to circuit impedance $Z= 6.2 - j*0.13 \Omega$ whereas the '1' state corresponds to $Z=-48 - j*3 \Omega$. (d) Output power at $2f_0= 808$ MHz where the '0' corresponds to no power (noise floor) and the '1' corresponds to power on the fundamental frequency being converted to the second harmonic.

It can be seen that the reflected power at fundamental frequency alternates from -52dBm to about -20dBm, which leads to a more than 30 dB contrast between the two states. Moreover, the wave generated from the fundamental at the second harmonic alternated between -40 dBm and no power at all, which means that even higher contrast is obtained.

Since the bias is injected from the same port as the RF, the shape of the bias voltage and modulation speed are affected by the low pass filter of the circuit. This can be easily improved by designing a high-speed bias switching circuit, but the analysis of the resulting behavior is of great interest: the variation of the bias voltage from 100mV to 200mV led to an out-burst of 15dB more 2nd harmonic power. This is due to the enhanced variation of tunnel diode resistance caused by the dynamic biasing (very similar to driving a mixer with a strong LO). Since this waveform is very easy to generate, it could be interesting to optimize the biasing waveform to enhance the harmonic backscattering operation.

V. CONCLUSION

This work has demonstrated a harmonic backscattering transponder that operates using a single nonlinear, negative resistance device. It can produce simultaneously a reflection at excitation frequency and convert some of the power to the second harmonic, enabling communication schemes usually forsaken due to inappropriate hardware. The circuit operates below 200mV, which is a critical improvement over transistor technology that needs a voltage ranging from 1 to 3.3 V to operate.

Moreover, by adjusting the tunnel diode bias voltage, it would be possible to reconfigure the circuit from injection locked self-oscillating mixer to reflection amplifier-frequency doubler, which opens even more applications in the low power, long distance, low cost IoT paradigm.

ACKNOWLEDGEMENT

This work has received financial support from the French State in the frame of the "Investments for the future" Programme IdEx Bordeaux, reference ANR-10-IDEX-03-02, and LabEx AMADEus (ANR-10-LABX-0042-AMADEUS).

REFERENCES

- [1] J. Kimionis, A. Georgiadis, A. Collado and M. M. Tentzeris, "Enhancement of RF tag backscatter efficiency with low-Power reflection amplifiers," *IEEE Trans. Microw. Theory Techn.*, vol. 62, no. 12, pp. 3562-3571, Dec. 2014.
- [2] F. Amato, H. M. Torun, and G. D. Durgin, "RFID backscattering in long range scenarios," *IEEE Trans. Wireless Commun.*, vol. 17, no. 4, pp. 2718-2725, Apr. 2018.
- [3] Fantuzzi, M. Del Prete, D. Masotti and A. Costanzo, "Quasi-isotropic RF energy harvester for autonomous long distance IoT operations," *2017 IEEE MTT-S Int. Microw. Symp.*, Honolulu, HI, 2017, pp. 1345-1348.
- [4] CHP Lorenz, S. Hemour, and K. Wu, "Physical mechanism and theoretical foundation of ambient RF power harvesting using zero-bias diodes," *IEEE Trans. Microw. Theory Techn.*, vol. 64, no. 7, pp. 2146-2158, Jul. 2016.
- [5] A. Boaventura, J. Santos, A. Oliveira and N. B. Carvalho, "Perfect isolation: dealing with self-jamming in passive RFID systems," *IEEE Microw. Mag.*, vol. 17, no. 11, pp. 20-39, Nov. 2016.
- [6] D. Allane, G. Andia Vera, Y. Duroc, R. Touhami and S. Tedjini, "Harmonic power harvesting system for passive RFID sensor tags," *IEEE Trans. Microw. Theory Techn.*, vol. 64, no. 7, pp. 2347-2356, July 2016.
- [7] V. Palazzi, F. Alimenti, P. Mezzanotte, G. Orecchini and L. Roselli, "Zero-power, long-range, ultra low-cost harmonic wireless sensors for massively distributed monitoring of cracked walls," *IEEE MTT-S Int. Microw. Symp.*, Honolulu, HI, 2017, pp. 1335-1338.
- [8] F. Amato, and S. Hemour, "The harmonic tunneling tag: a dual band approach to backscattering communication" *IEEE Int. Conf. RFID Technol. Application*, Pisa, Italy Sep. 2019.
- [9] CHP Lorenz, S. Hemour, W Li, Y Xie, J Gauthier, P Fay, and K. Wu, "Breaking the efficiency barrier for ambient microwave power harvesting with heterojunction backward tunnel diodes" *IEEE Trans. Microw. Theory Techn.*, vol. 63, no. 12, pp. 4544-4555, Dec. 2015.
- [10] P. Paletti, R. Yue, C. Hinkle, S.K. Shirey, and A. Seabaugh, "Two-dimensional electric-double-layer Esaki diode" *npj 2D Mater Appl* **3**, 19 (2019)
- [11] N.-C. Kuo, B. Zhao, and A. M. Niknejad, "Inductive power transfer uplink using rectifier second-order nonlinearity," *IEEE Trans. Circuits Syst. I, Reg. Papers*, vol. 63, no. 11, pp. 2073-2085, Nov. 2016.
- [12] Y. Zhao, S. Hemour, T. Liu, and K. Wu, "Negative resistance based electronic impedance tuner," *IEEE Microw. Compon.Lett.*, vol. 28, no. 2, pp. 144-146, Feb. 2018.